The in Vitro and in Vivo Antitumor Effect Associating With the Hippo-yap Signaling Pathway of Gallic Acid and Its Combination With Icotinib Hydrochloride on the Non-small Cell Lung Cancer Cellular and Xenograft Tumor-bearing Nude Mouse Models

Dapeng Wang
Chinese PLA General Hospital https://orcid.org/0000-0001-6193-098X
Yinghua Guo
PLAGH: Chinese PLA General Hospital
Yuan Liu
PLAGH: Chinese PLA General Hospital
Bin Zhang
Binzhou Medical College: Binzhou Medical University
Po Bai
PLAGH: Chinese PLA General Hospital
Xiaolei Su
PLAGH: Chinese PLA General Hospital
Xuege Jiang
PLAGH: Chinese PLA General Hospital
Sarengerile Han
Inner Mongolia Medical College: Inner Mongolia Medical University
Tingzheng Fang
Chinese PLA General Hospital
Xuelin Zhang
Chinese PLA General Hospital
Junfeng Wang
Chinese PLA General Hospital
Changting Liu (changtingliu1212@sohu.com)
https://orcid.org/0000-0002-5346-2140

Research

Keywords: Gallic acid, Icotinib hydrochloride, NSCLC, Combination therapy, Hippo-YAP

Posted Date: June 16th, 2021

DOI: https://doi.org/10.21203/rs.3.rs-618568/v1

Abstract

Background: Epidermal growth factor receptor tyrosine kinase inhibitors (EGFR-TKIs) have been widely used as first-line therapy for patients with EGFR mutant non-small cell lung cancer (NSCLC). However, EGFR-TKIs treatment of NSCLC will inevitably produce acquired drug resistance. It greatly limits the therapeutic effect of TKI. Recent studies have found that some natural drugs combined with TKI in the treatment of NSCLC may not only improve the efficacy but also reduce the occurrence of acquired drug resistance. This study intends to investigate the inhibitory effect of Gallic acid, (a natural plant extract) combined with EGFR-TKI on the growth of NSCLC cell lines and xenograft tumor-bearing nude mouse models and its possible mechanism.

Methods: Immunohistochemical method was used to detect the expression of Caspase-3, Caspase-9, Bcl-2, Cox-2, YAP and p-YAP in tissues of human non-small cell lung cancer (NSCLC). NSCLC cell lines A549 and PC9 were co-cultured with Gallic acid and / or Icotinib hydrochloride to test the antitumor effect. Cell proliferation was measured by MTT assay. In addition, apoptosis was measured by flow cytometry (FCM). In addition, intracellular calcium concentration in A549/PC9 cells was detected by calcium fluorescence probe. Besides, cell migration was detected by Transwell assay. Moreover, expression of related key genes was detected by qPCR, and expression of Caspase-3, Caspase-9, Bcl-2, Cox-2, YAP and p-YAP was determined by Western blotting. The anticancer effect of Gallic acid combined with Icotinib hydrochloride *in vivo* was studied by xenograft tumor-bearing nude mouse models.

Results: 6 cases of human non-small cell carcinoma were analyzed by immunohistochemical staining. As a result, the expression of Caspase-3, Caspase-9, Bcl-2, Cox-2, YAP protein in lung cancer tissues was lower than that in normal tissues. However, the expression of p-YAP protein in cancer tissues was higher than that in normal tissues; MTT analysis showed that Gallic acid had a good inhibitory effect on NSCLC. A549 and PC9 cells in a concentration-dependent manner; Gallic acid combined with Icotinib hydrochloride significantly decreased the cell survival rate compared with single drug intervention. Treatment with Gallic acid and/or Icotinib hydrochloride induced apoptosis, accompanied by increased expression of Caspase-3, Caspase-9, Bcl-2, Cox-2 and YAP, and inhibited cell migration by down-regulating p-YAP. Gallic acid combined with Icotinib hydrochloride significantly increased the concentration of intracellular Ca^{2+} compared with the control group. The involvement of Ca^{2+} in the process of apoptosis may be related to p-YAP, which may be the key to the apoptosis of lung cancer cells induced by Gallic acid combined with Icotinib hydrochloride. Gallic acid combined with Icotinib hydrochloride promoted apoptosis of A549 and PC9 cells by down-regulating the expression of phosphorylated YAP. Dephosphorylation of signal transduction leads to the formation and activation of YAP and enhances the anti-proliferation response. The combined administration of Gallic acid and Icotinib hydrochloride inhibited the growth of tumor and decreased the expression of p-YAP in the xenograft tumor-bearing nude mouse models.

Conclusion: Gallic acid may enhance the proliferation inhibition and apoptosis induction effect of Icotinib hydrochloride on lung cancer cell lines. Besides, Gallic acid combined with Icotinib hydrochloride may be

a potential treatment in the treatment of NSCLC. In addition, Gallic acid is promising as a potential antineoplastic drug in the treatment of lung cancer.

Background

Lung cancer is one of the most common malignant tumors. Lung cancer has become the malignant tumor with the highest morbidity and mortality in the world since the 1990s.[1] With the progress of science and technology, the limitations of surgical treatment and the side effects of chemotherapy drugs make the 5-year survival rate of patients less than 20% though the techniques of surgery, radiotherapy and chemotherapy have been improved.[2] Molecular targeted therapy has become another important choice for patients with non-small cell lung cancer(NSCLC), and to some extent improve the survival rate of patients with NSCLC with the application and development of tumor molecular biology and genomics. However, there are no mutations in the corresponding targeting genes or acquired drug resistance to targeted drugs in some patients, which greatly reduces the clinical application of targeted drugs. As a result, the prognosis of NSCLC patients is still not optimistic. As a consequence, people begin to explore the combined use of targeted drugs and other drugs in preclinical studies, which is of great significance for prolonging the survival time of patients with non-small cell lung cancer.

In recent years, many drugs extracted from natural plants have attracted attention because of their obvious pharmacokinetic characteristics and mild side effects with the deepening of traditional Chinese medicine research. Gallic acid (GA, Figure 1) is a natural phenolic compound, and is a plant extract, which is rich in tea, grapes, nuts and red wine.[3] It is reported that it has a variety of pharmacological and biological properties, including antibacterial activity[4], antiviral activity[5] and antioxidants.[6] More attention has been paid to the anti-tumor function of GA in recent years. Studies have shown that GA may inhibit the growth of malignant tumors by inhibiting the proliferation and invasive activity of tumors.[7-11] Studies have shown that GA has a good inhibitory effect on cervical cancer,[12] breast cancer,[11] lung cancer,[13] prostate cancer[14] and other tumors. It was speculated that Gallic acid combined with tyrosine kinase inhibitors may have a good inhibitory effect on NSCLC.

Icotinib hydrochloride (IH, Figure1) is a small molecular tyrosine kinase inhibitor independently developed in China. It is a highly efficient and specific epidermal growth factor receptor tyrosine kinase inhibitor (EGFR-TKI). In clinic, IH has been widely used in China, and its clinical efficacy is similar to that of gefitinib.[15] IH has similar clinical efficacy and higher safety compared with gefitinib.[16]

The effects of GA combined with IH on NSCLC cells and xenograft tumor-bearing nude mouse models were investigated. The better efficacy of the combination of GA and IH has not been confirmed by large-scale clinical trials though the clinical application of IH has been relatively mature. Through the combined use of GA and IH, the effects of combined intervention on the biological characteristics of NSCLC *in vivo* and *in vitro* were observed, and the related mechanisms were discussed, so as to provide ideas and experimental basis for clinical practice.

Methods And Materials

Materials and reagents

The human NSCLC A549 and PC9 cell lines were obtained from the Hunan Fenghui Biotechnology Co., Ltd (Hunan China), and the cells were maintained in RPMI 1640 (Thermo Fisher Scientific, Waltham, MA, USA) supplemented with 10% fetal bovine serum (Thermo Fisher Scientific) and 100 mg/mL penicillin/streptomycin (Solarbio, Beijing, China) at 37°C in a humidified atmosphere with 5% CO_2. GA was purchased from Sigma-Aldrich Chemical Co. (St. Louis, MO, USA). of purity above 98%. IH was kindly provided by Zhejiang Beta Pharma Co., Ltd. (Zhejiang, China) and dissolved in 100%. Fetal bovine serum (FBS) and RPMI-1640 medium were purchased from Gibco-BRL (Grand Island, NY, USA) supplemented with 10% fetal bovine serum (Thermo Fisher Scientific) and 100 mg/mL penicillin/streptomycin (Solarbio, Beijing, China) at 37°C in a humidified atmosphere with 5% CO_2. The cell apoptosis detection kit with Annexin V-fluorescein isothiocyanate (FITC)/propidium iodide (PI), was purchased from Beyotime Institute of Biotechnology (Jiangsu, China). Primary antibodies against Bcl-2, Yap, p-Yap, Cappase-3, Caspase-9, and β-actin were purchased from Santa Cruz Biotechnology, Inc. (Santa Cruz, CA, USA). Anti-rabbit IgG peroxidase-conjugated secondary antibody, sodium salt (SDS)-polyacrylamide gel electrophoresis (SDS-PAGE) gels, and polyvinylidene difluoride (PVDF) membrane were purchased from Amersham Biosciences (Piscataway, NJ, USA).

Patients

6 cases of primary lung cancer and 6 cases of normal lung tissue (near cancer) from June 2019 to September 2019 were collected from the Department of Pathology, Chinease PLA General Hospital. There were 4 males and 2 females, who aged from 42 to 68 years old, with an average age of (59.24 ±5.76) years. Histological type: adenocarcinoma; All selected patients underwent radical resection without chemotherapy or radiotherapy before operation. The study was approved by the hospital ethics committee.

Cell Culture

Human NSCLC A549 and PC9 cell lines were obtained cultured in RPMI-1640 medium containing 10% FBS at 37℃ in a humidified 5% CO_2 incubator. Change the medium 2~3 times every week and the cells were used in their logarithmic growth phase; try trypsin digestion and passage.

Human lung tissue immunohistochemistry

Tissue specimens were fixed in 10% neutral formalin solution for 24h□48h, embedded in conventional paraffin, 3μm serial sections, baked slices in 60℃ oven for 30min, dewaxing, antigen retrieval, antigen exposure, sealing, dripping peroxide. The operation steps of enzyme blocker, dripping of the secondary antibody, DAB color development, etc. were carried out according to the operating instructions of the Roche automatic immunohistochemistry instrument. The primary antibody dripped manually, and finally,

it was counterstained with artificial hematoxylin, blue back, and sealed with a neutral gum sheet. The primary antibody of immunohistochemistry was rabbit anti-human Caspase-3、Caspase-9、Bcl-2, Cox-2, YAP, p-YAP polyclonal antibody (1: 200, Santa Cruz, USA). Immunohistochemical staining scoring standard: judged by the intensity of nuclear staining or cytoplasm staining in tumor tissue area and normal tissue area. The widely accepted German semi-quantitative scoring system was used to score staining intensity and extent in different areas. Each specimen was assigned a score according to the intensity of the nuclei, cytoplasmic, and membrane staining (no staining¼0; weak staining¼1, moderate staining¼2, and strong staining¼3) and the extent of stained cells (0–5%¼0, 5–25%¼1, 26–50%¼2, 51–75%¼3 and 76–100%¼4). The final immunoreactivity score was determined by multiplying the intensity score by the score for the extent of stained cells, generating a score that ranged from 0 (the minimum score) to 12 (the maximum score).

Cell viability assay

According to the manufacturer's instructions, cell viability was evaluated using MTT (Solarbio, Beijing, China). Briefly, cells were seeded into 96-well plates at 8×10^3cells per well and cultured for the indicated time points. Ten microlitres of MTT (Preparation concentration: 5mg/ml) solution was added into the culture medium in each well. After a 4 hr incubation, use a 1ml pipette to remove the supernatant from each well. Be careful not to aspirate crystals at the bottom of the well. Add 100μl DMSO to each well. Incubate with shaking at room temperature for 15 minutes. OD values were read using a microplate reader (Bio-Tek Company, Winooski, VT) at a wavelength of 490nm. Each time point was repeated in three wells, and the experiment was independently performed three times.

Cell apoptosis assay

Cell apoptosis was evaluated by flow cytometry using an Annexin V-FITC Apoptosis Detection Kit (KeyGen Biotech Co. Roche, Nanjing, China). Briefly, cells were seeded into 24-well plates at 5×10^5 cells per well and cultured for 48 hr. Then the cells were detached by trypsinization, washed twice in PBS (2000 r.p.m., 5 min), and resuspended in 500 ml binding buffer. A volume of 5μl Annexin V-FITC and 10μl propidium iodide was added and mixed gently, and the cells were stained in the dark for 10 min at room temperature. The cells were analyzed immediately by flow cytometry (BD FACSCalibur, BD. Bioscience, San Diego, CA) and analyzed using FLOWJO software (FlowJo, Ashland, OR). On the flow cytometer, the Annexin V-FITC (Ex=488nm; Em=530nm) was detected through the FITC channel and the PI is detected through the PE detection channel. Result interpretation: Upper left area: late apoptotic or dead cells; upper right area: metaphase apoptotic cells; lower left area; normal cells; lower right area: early apoptotic cells. The experiment was repeated three times.

Cell morphology

Take the cells in the logarithmic growth phase, wash, count, and resuspend the cells. The cells are seeded in a six-well plate with 2×10^5cells per well. Use a micropipette to add RPMI1640 complete medium to each well. Gently shake the six-well plate, mix the cells in the six-well plate, observe whether the cells are

evenly distributed under a microscope, and place them in a cell incubator (temperature: 37℃, containing 5% CO_2). Cultivate the cells until they are in the logarithmic growth phase, add RPMI1640 complete medium containing intervention factors, and place them in a cell incubator (temperature: 37°C, containing 5% CO_2) for 48 hr. Take out the six-well plate and observe the changes in cell morphology and number under a light microscope.

Transwell migration assay

The ability of cell migration was measured by Transwell. The cells in logarithmic growth phase were taken and the cell density was adjusted to 5×10^5 cells / ml. In addition, 200μL cell suspension was put into the upper chamber of Transwell cells, and then 600μL complete medium (including intervention drugs) was added to the lower chamber of 24-well culture plate. The culture plate was placed in a CO_2 incubator at 37 ℃ for 48 hr. It was took out the Transwell, and washed twice with PBS. In addition, the matrix glue and the cells in the chamber were wiped off with a cotton swab. Moreover, it was soaked in 70% methanol for 30min and 60min, and dyed with crystal violet. After crystal violet staining, the stained migrating cells can be decolorized with 33% acetic acid, crystal violet can be completely eluted, and then the OD value of the eluent at 570nm was determined by enzyme labeling instrument, which indirectly reflected the number of migrating cells. The experiment was repeated at least three times.

Flow cytometry analysis to determine $[Ca^{2+}]$ i

2×10^4 of A549 and PC9 cells, add different intervention drugs, after 48hr, collect cells were rinsed with PBS. They were then loaded with 0.5 ml of 2μM Furo-4AM, at room temperature for 60 min, and subsequently rinsed twice with PBS. Cells were then analyzed using a BD Aria flow cytometer (BD Bioscience, San Jose, CA, USA). The experiment was repeated at least three times.

Real-time qPCR (qPCR)

Take logarithmic growth cells, inoculate them in a 6-well plate at 2×10^5/L, place them in an incubator for 24 hr, add different intervention drugs (control group, GA group, IH Group, GA combined with IH group). After 48 hr of treatment, cells were collected, total RNA was extracted. ACTB was used as an internal reference gene to detect the expression of Caspase3, Caspase9, Bcl-2, Cox-2, and YAP (Table 1). The $2^{-\triangle\triangle}$Ct method was employed to determine the relative mRNA expression.

Western blot analysis

Western blot was performed with mouse monoclonal antibody against Caspase3, Caspase9, Bcl-2, Cox-2, YAP、p-YAP, and the secondary antibody was goat anti-mouse immunoglobulin G-horseradish peroxidase (IgG-HRP) conjugate. SDS-PAGE concentrate gel 4%, separation gel 12%. Protein Marker (SM26616, Thermo Fermentas, USA). Load 30 μg per lane. First, electrophoresis at 90V for 30min, and then electrophoresis at 120V for 2h. 300mM, transfer membrane for 2h. Fast blocking solution without protein (#W1028, SinoGene, China) for 3-5 minutes; add the primary antibody anti-Caspase-3, Caspase-9, Cox-2,

Bcl-2, YAP, p-YAP (1:1000) at room temperature for 1 hr. Wash with TBST 3 times, 10 min each time. After that, the secondary antibody (1:3000) was incubated for 1 hr, washed twice with TBST, and finally washed once with TBS for 10 minutes each time. On the cling film, lay the film flat, add ECL luminescent solution (29050, Engreen, China), and then expose and test in the darkroom. Beta-actin (1:3000, AC028, Abclonal, China) restandard internal reference.

Animal study

A total of 24 BALB/C nude mice (4 weeks old, weighing 18–22 g) were purchased from the Experimental Animal Center. The study was approved by the Research Ethics Committee of the Chinease PLA General Hospital. Under sterile conditions, 0.2ml (PC9) of cell suspension (I×10^7cells/mL) was pipetted with a 1 mL disposable syringe and slowly injected into the right armpit of the nude mouse. The long diameter of the tumor block >1 mm and felted lumps was indicative of the successful establishment of the NSCLC mouse model. After successful modeling, control group, GA group (30μg/kg), IH group (100mg/kg), combined treatment group(30μg/kg+100mg/kg). Continuous administration for 14 d (1 time/d). During the administration, the long diameter and short diameter of the transplanted tumors were measured by vernier calipers every 3d, repeated in triplicate to obtain the average values. The tumor volume was then calculated: V = long diameter × short diameter^2/2, and the growth curve of the transplanted tumors were plotted based on the values obtained. Each mouse was heparinized by intraperitoneal injection of 0.5% heparin (0.5mL), and then eye blood samples were collected to measure the levels of serum alanine aminotransferase (ALT) and alkaline phosphatase (ALP), blood urea nitrogen (BUN) and creatinine (Cr) after the last administration on the 14th day. In addition, the animals were euthanized with carbon dioxide asphyxiation, the tumor was removed, and the volume of the tumor was measured after weighing the animals. In addition, the expression of Caspase-3, YAP and p-YAP protein in tumor tissue was detected by immunohistochemical staining, and the percentage of Caspase-3, YAP and p-YAP protein positive staining was quantified by optics. A microscope (IX51Olympus, Japan) and Image Pro Plus software were adopted to take photos and analyze slides. The standard method of immunohistochemical staining was judged according to the intensity of nuclear staining or cytoplasmic staining in tumor tissue area and normal tissue area.

Statistical analysis

The quantitative experiments were performed in triplicates, and the data were represented as the mean ± standard deviation (S.D.). A statistical comparison of the data was conducted using a two-tailed Student's t-test. Statistical significance between the two groups was defined as $p \leq 0.05$.

Results

Expression of key genes in human NSCLC and paired adjacent normal lung tissues

First of all, the expression of Caspase-3, Caspase-9, Bcl-2, Cox-2, YAP and p-YAP in 6 NSCLC specimens were analyzed. The scoring standard of immunohistochemical staining was used. As shown in Figure 2

and Table 2, both Caspase-3, Caspase-9, Bcl-2, Cox-2 and YAP were expressed in normal lung tissues, but not or weakly expressed in NSCLC tissues. Compared with normal lung tissue, more p-YAP expression was detected in NSCLC tissue. In immunohistochemical staining, the positive granules were yellow or brown. All of them were located in the nucleus, and were granular, dispersed and / or mixed (Figure 2).

Inhibitory effect of GA, IH and combination on A549 / PC9 cells

MTT assay was used to detect the growth of A549/PC9 cell lines treated with different concentrations of GA, IH alone and in combination groups. This study intends to investigate the anti-tumor effect of GA and whether GA may promote the inhibitory effect of IH on these two lung cancer cell lines. As a result, when GA reached 132μM, the growth of A549 and PC9 cells were inhibited (Figure 3 a-b). IH could inhibit the proliferation of A549 and PC9 cells. However, only 0.5μM IH could significantly inhibit the proliferation of PC9 cells because of the different sensitivity of the two cells (Figure 3 d). However, A549 cells had an inhibitory effect only when the concentration of IH reached 5μM (Figure 3 c). These results showed that IH had a greater effect on EGFR mutant cell line (PC9) than on wild type EGFR cell line (A549). It may be seen from the combination group. The concentration of IH in PC9 cells reached 0.5μM, or the concentration of IH in A549 cells reached 5μM, the cell proliferation was significantly inhibited when the concentration of GA reached 132μM, indicating that both GA and IH had synergistic inhibitory effects on these two types of cells (Figure 3 e-f). At the same drug concentration, GA or IH or combined treatment could significantly inhibit the proliferation of A549/PC9 cells. The combination of the two drugs showed excellent synergistic effect for these two kinds of cells.

Effects of GA, IH and combined treatment on the morphology of A549 / PC9 cells

The results of MTT assay confirmed that the combination of GA and IH had obvious inhibitory effect on A549/PC9 cells. The combination of 5μM / 0.5μM IH and 132μM GA showed a good synergistic effect on A549/PC9 cells according to the results of MTT. It did not show a stronger inhibitory effect on tumor cells with the increase of GA concentration. As a consequence, A549 (132μM GA + 5μM IH) and PC9 (132μM GA + 0.5μM IH) were chosen for follow-up experiments. As a result, compared with the control group, GA, IH and the combination group increased the number of apoptotic cells in A549/PC9 of lung cancer cells. The apoptotic lung cancer cells were mainly round and exist in one or more crispy slices, and fell off from the cell mass and suspend in the culture medium. The size of the apoptotic lung cancer cells was smaller than that of tumor cells. Besides, the cell structure was not clear (Figure 4 a-d ×10， e-h ×20).

Inducing effect of GA, IH and combination on apoptosis of A549 and PC9 cells

AnnexinV / PI staining and flow cytometry were adopted to detect the apoptosis rate in order to study whether GA, IH and the combination of GA and IH can induce apoptosis in A549 and PC9 cells. The results showed that the apoptosis rate in the combination group (30.93% / 33.54%) was significantly higher than that in the GA (17.59% 17.55%) and IH (27.31% / 32.32) groups in the A549 / PC9 cell group (Figure 5 a-b, * $P < 0.05$， ** $P < 0.01$， *** $P < 0.001$). As a result, the inhibition of cell growth by GA and IH may be related to the induction of apoptosis.

Effects of GA, IH and combined treatment on migration of A549 and PC9 cells

It was detected by Transwell test in order to study the effect of GA, IH and combination therapy on the migration of A549 and PC9 cells. The absorbance of acetic acid solution was read by enzyme labeling instrument (570nm). The results showed that the three treatment groups had significant inhibitory effects on the migration of A549 and PC9 cells. In addition, the combination group significantly inhibited the migration of lung cancer cells compared with the single drug group (Figure 6 a-b).

Effect of apoptosis induced by GA, IH and combined treatment on $[Ca^{2+}]$ i in A549 / PC9 cells

We speculate that Ca^{2+} as the second messenger may be involved in mediating the apoptosis of A549/PC9 cells induced by GA and IH. The results showed that with the increase of A549/PC9 cell apoptosis, the intracellular calcium concentration increased (Figure 7 a-b), indicating that Ca^{2+} may participate in the process of GA and IH-induced apoptosis.

Effects of GA, IH and combined treatment on mRNA expression of key genes in A549 and PC9 cells

The mRNA expression levels of key genes in A549 and PC9 cells were analyzed by qPCR assay. As a result, compared with the control group, the expression levels of Caspase3, Caspase9, Cox-2, Bcl-2 and YAP were increased in both the single drug group and the combination group, especially in the combination group (Figure 8 a-b).

Regulation of apoptosis and YAP pathway in A549 and PC9 cells by GA, IH and combined treatment

The protein expression of Caspase3, Caspase9, Bcl-2, Cox-2, YAP and p-YAP after different intervention was detected in order to further verify whether the effects of GA, IH and combined drugs on A549/PC9 are involved in the regulation of YAP-related pathways and the relationship between YAP protein and tumor cell apoptosis. The results showed that the expression of Caspase3, Caspase9, Bcl-2, Cox-2, p-YAP/YAP in the combination group was significantly higher than that in the control group (Figure 9 a-b). However, the level of single drug in the GA group was similar to that in the IH group. This study showed that the expression level of YAP protein in the combination group was significantly higher than that in the single treatment group with statistical significance (Figure 9 a-b). This suggested that DNA repair is blocked and may induce apoptosis. These results suggested that YAP signal pathway may be involved in regulating the anti-tumor effect of Gallic acid on A549 and PC9; GA, IH and combination groups may produce anti-tumor effect by inhibiting the phosphorylation of YAP; GA may promote apoptosis through YAP signal pathway and enhance the anti-tumor effect of IH.

Effects of GA, IH and combined treatment on xenograft model in PC9 mice

The effects of GA, IH and the combination group on the growth of xenograft subcutaneously with PC9 in mice were examined. Compared with the control group either the single drug group or the combination group could significantly inhibit the growth of the xenograft tumor-bearing nude mouse models and significantly reduce the tumor volume (Figure 10 a-b; Table 3). Compared with the two monotherapy

groups, the tumor growth in the combination group was more significantly inhibited (Figure 10 a-b; table 3). In addition, the degree of phosphorylation of YAP and the expression of YAP, Caspase-3 protein in the xenograft model tumor tissue of mice treated with GA, IH and GA combined with IH were detected by immunohistochemical analysis. As a result, compared with the control group, the expression of p-YAP decreased and the expression of YAP, Caspase-3 protein increased in tumor tissues of mice treated with GA, IH and combined drugs (Figure 11 a-c). Compared with the single drug group, the expression of YAP, Caspase-3 protein in the combination group was higher than that in the single drug group. The effects of GA, IH and GA combined with IH on liver and kidney function in nude mice were further observed (Table 4). Generally speaking, GA plays an inhibitory role in tumor growth of NSCLC. GA may enhance the anti-tumor effect of IH by inhibiting the phosphorylation of YAP.

Discussion

As one of the most common types of cancer, lung cancer is characterized by high mortality. NSCLC is easy to develop drug resistance in the process of treatment. As a consequence, it is difficult to choose the best treatment.[17] GA has been extensively studied in anti-tumor, immunomodulatory, anti-inflammatory and other aspects.[3] The combination of GA and chemotherapeutic drugs may improve the therapeutic effect of chemotherapeutic drugs or improve the sensitivity of chemotherapeutic drugs to drug-resistant cells.[18] However, the use of chemotherapeutic drugsis limited by their side effects, including hepatorenal toxicity and gastrointestinal reactions.[19] Tyrosine kinase inhibitor (TKI) is a drug that inhibits the activity of tyrosine kinase. IH is an EGFR-TKI used to treat NSCLC. It may compete with adenosine triphosphate (ATP) to inhibit the activation of EGFR.[20] We shifted the focus from chemotherapeutic drugs to target drugs to explore the synergistic effect and possible mechanism between GA and EGFR-TKI because the target drugs almost act on specific sites.

The combined effect of IH and GA at different concentrations by MTT were evaluated. As a result, GA and IH could inhibit the proliferation of A549 and PC9 cells in a concentration-dependent manner. The combination of different concentrations of IH and GA has a synergistic inhibitory effect on tumor cells. Interestingly, increasing the concentration of GA had little effect on A549 and PC9 cells in the combination. These two compounds did not produce more significant anti-tumor effect. It is likely that the concentration of the two compounds has been saturated. The combined effect of A549 and PC9 cells at lower concentrations of GA and IH were also studied. However, the results did not show a significant inhibitory effect on tumor cells, and had no practical significance because the cell inhibition rate was too low. As a consequence, the combination of relatively high concentrations of GA and IH is a better choice for the combination of A549 and PC9 cells according to our experimental results. According to the results of apoptosis, it was found that the two drugs showed a good synergistic effect of inhibiting proliferation and inducing apoptosis in lung cancer cell lines. In the combined treatment group, Caspase-3 and-9 splices increased significantly, indicating that the combination of the two drugs induced the occurrence of Caspase cascade. The increase of Bcl-2 protein level indicates that mitochondria may play an important role in the process of apoptosis. Compared with the single drug group, the expression of Cox-2

protein in the combination group was significantly increased, indicating that the biosynthesis of prostaglandins increased in the process of apoptosis. Studies have shown that Cox-2 may drive tumorigenesis by producing prostaglandins (Chen et al., 2020). It was unexpectedly found that YAP and Cox-2 did not promote the proliferation of NSCLC A549 and PC9 cells, which may be related to the diversity and complexity of tumors. YAP signal transduction pathway is a classical signal transduction pathway in NSCLC, which may regulate cell growth activity. We studied the downstream pathway of YAP in order to study the mechanism of the combination of GA and IH on NSCLC cell line. Western blot results showed that the combination of GA and IH could inhibit the decrease of p-YAP expression and increase the expression of pro-apoptotic factor Bcl-2. As a result, the binding of GA to IH can cause the degradation of YAP and its downstream proteins and promote apoptosis. As a compensation mechanism of EGFR-TKIs, it may partly explain its synergistic effect with GA and IH.

According to the previous studies, the main signal pathways involved in apoptosis include endogenous apoptotic pathways, exogenous apoptotic pathways and endoplasmic network pathways.[21] However, the understanding of how GA induces apoptosis is still limited. The mechanism of apoptosis induced by GA in lung cancer cells is still unclear. As a consequence, it is speculated that these three pathways play an important role in the apoptosis of lung cancer cells induced by GA. Two kinds of NSCLC cells (A549 and PC9) were studied. It laid a theoretical foundation for the application of GA in anti-tumor by observing the inhibitory effect of GA on NSCLC cells and the biological mechanism of regulating apoptosis of NSCLC cells. GA, IH and the combination group increased [Ca^{2+}] levels in A549 and PC9 cell lines. The disruption of the dynamic balance of Ca^{2+} is considered to be the key to apoptosis.[22] In fact, the decrease of p-YAP gene expression may disrupt Ca^{2+} homeostasis, resulting in significant apoptosis observed in this study. YAP is a sensor that affects tumor microenvironment structure and mechanical signals and mediates downstream inhibitory contact with E-cadherin.[23] The experiments showed that GA and IH induced the migration of NSCLC cells in Transwell experiment and played a role in promoting apoptosis. It was speculated that the possible explanation for this migration is that the increase of Ca^{2+} mediated by Hippo-YAP channel may reduce the migration of A549 and PC9 cells by regulating local cadherin. More specific studies are needed to evaluate the relationship between the invasion of lung cancer cells mediated by these drugs and the activation of Ca^{2+} signaling pathway. As a result, Ca^{2+} and YAP phosphorylation are related to a certain extent, which may be that p-YAP-mediated Ca^{2+} enters lung cancer cells and causes apoptosis. It is necessary to further study how Ca^{2+} stored in lung cancer cells enter the cells to induce YAP phosphorylation and provide another way for lung cancer treatment and intervention.

Hippo signaling pathway is closely related to cell development, proliferation, apoptosis anddifferentiation. It has attracted great attention because it is involved in tumor migration and metastasis.[24,25] As a downstream signal molecule of Hippo signaling pathway, YAP may be involved in cell proliferation and apoptosis.[26,27] As an important signal pathway involved in tumorigenesis and development, Hippo-YAP signaling pathway plays an important role in regulating organ size and maintaining the dynamic balance of cell proliferation and apoptosis. The study showed that the

immunohistochemical detection of p-YAP in non-small cell lung cancer was strongly positive. However, the expression in normal lung tissue was negative. As a consequence, it was inferred that YAP plays an important role in the occurrence and development of non-small cell lung cancer. The exploration of the molecular mechanism of YAP is helpful to reveal the role of YAP in the pathogenesis of non-small cell lung cancer. This suggests that YAP-activated Hippo pathway is involved in the development of non-small cell lung cancer. Hippo signal transduction pathway is the way to inhibit cell growth. It mainly mediates the inhibition of cell-to-cell contact and plays a key role in maintaining organ size and the balance between cell proliferation and apoptosis. It was speculated that the effect of Gallic acid on non-small cell lung cancer may be related to the Hippo pathway. GA may activate Hippo signal pathway, inactivate carcinogen p-YAP, and cannot initiate the expression of downstream tumor-promoting target genes, thus enhancing the anticancer effect of IH on non-small cell lung cancer. However, studies have shown that the high expression of YAP in colorectal cancer and hematological diseases is positively correlated with the growth of cancer cells. However, the authors analyzed the TGGA database and found that there was no negative correlation between YAP and Cox-2 in various human lung cancers. There is no doubt that this is related to the diversity and complexity of tumor patient samples. These findings also suggest that attention was paid more to the function of gene expression in YAP studies.

It was confirmed that the combination of GA, IH and the combination group could inhibit the growth of xenograft tumor-bearing nude mouse models in the *in vitro* experiment. Compared with the control group, both the single drug group and the combination group could inhibit the growth of transplanted tumor and inhibit the reduction of tumor volume (Figure 10 a-b; Table 3). Compared with the two single drug groups, the combination group inhibited the tumor growth more significantly, with statistical significance (Figure 10 a-b; Table 3). The expression of related proteins Caspase-3, YAP and p-YAP was detected by immunohistochemical method. As a result, both the single drug group and the combination group decreased the phosphorylation level of YAP and increased the expression of YAP and caspase-3 protein in the xenograft tumor tissue of mice. The effects of Gallic acid treatment on liver and kidney function in nude mice were further observed (Table 4). This treatment shows good biological safety and tolerance in the transplanted tumor model, which also provides a certain reference for the combined application of GA and IH in the clinical treatment of patients with NSCLC. There may be a relationship between the binding ability of GA and IH and the combined effect from the combined data of GA and IH combined drugs. GA contains six-membered ring structure, oxygen-containing functional groups and unsaturated bonds. It was speculated that these characteristics may be related to its affinity to EGFR. In other words, IH and GA may form a more stable complex and produce a synergistic effect. Although no more specific binding conditions are mentioned in this paper, the experimental results suggest that GA may bind to EGFR in the cell membrane to play a synergistic effect. The relationship between the two drugs and EGFR phenotype is worthy of further study, and more EGFR phenotypes should be considered for further verification though the synergistic effect of the two drugs has been found through the experimental results.

Conclusions

This study confirmed for the first time that GA inhibits the proliferation and induces apoptosis of NSCLC A549 and PC9 cells in a dose-dependent manner by regulating Hippo-YAP signal pathway. It is worth mentioning that the results of this study show that GA regulates the expression of downstream apoptotic molecules by blocking the phosphorylation of YAP and plays an auxiliary role in the anticancer activity of IH. However, further studies are needed to clarify the role of GA in other potential apoptotic pathways. Corresponding clinical trials should be carried out in order to confirm the anticancer effect of GA on NSCLC and its sensitizing effect on EGFR-TKIs.

Abbreviations

NSCLC: non-small cell lung cancer; GA: Gallic acid; IH: Icotinib hydrochloride; EGFR-TKi: epidermal growth factor receptor tyrosine kinase inhibitor

Declarations

Acknowledgements

The authors would like to thank Professor Chengbin Cui for critically reviewing the manuscript.

Authors' contributions

Dapeng Wang, Yinghua Guo and Yuan Liu performed the experiments, analyzed the data, prepared figures and/or tables, and authored or reviewed drafts of the manuscript. Bin Zhang, Po Bai and Xiaolei Su performed the experiments and contributed reagents/materials/analysis tools. Xuege Jiang, Sarengerile Han, Tingzheng Fang and Xuelin Zhang performed the experiments and prepared figures and/or tables. Junfeng Wang conceived and designed the experiments, authored or reviewed drafts of the manuscript, and approved the final manuscript draft. Changting Liu conceived and designed the experiments, authored or reviewed drafts of the manuscript, and approved the final manuscript draft.

Availability of data and materials

Not applicable.

Ethics approval and consent to participate

The current study was performed with the approval of the Ethics Committee of the the Chinese PLA General Hospital. Participants have signed an informed consent form (ICF).

Consent for publication

The authors affirm that human research participants provided informed consent for publication of their data.

Competing interests

The authors declare that they have no conflicts of interest.

Funding

This work was supported by the Postdoctoral Science Foundation(2017T100809); the Key Program of Logistics Research (BWS17J030).

Author details

[1]Department of Respiratory and Critical Care Medicine, The Second Medical Center & National Clinical Research Center for Geriatric Disease, Chinese PLA General Hospital, Beijing, China

[2]Department of Emergency, Outpatient Department, The Second Medical Center & National Clinical Research Center for Geriatric Disease, Chinese PLA General Hospital, Beijing, China

[3]College of Pulmonary and Critical Care Medicine, The Eighth Medical Center, Chinese PLA General Hospital, Beijing, China

[4]Respiratory Diseases Department and Critical Care Medicine, Binzhou Medical University Hospital, Binzhou, China

[5]Respiratory Diseases Department, PLA Rocket Force Characteristic Medical Center, Beijing, China

[6]Department of Interventional Oncology, Inner Mongolia International Mongolian Hospital, Huhehaote, China

ETHICS STATEMENT

The current study was performed with the approval of the Ethics Committee of the the Chinese PLA General Hospital. The study participants gave consent to have their data published.

CONSENT FOR PUBLICATION

Written informed consent for publication was obtained from all participants.

AVAILABILITY OF DATA AND MATERIALS

All data generated or analysed during this study are included in this published article and its supplementary information files

CONFLICT OF INTERESTS

The authors declare no conflict of interest.

FUNDING

This work was supported by the Postdoctoral Science Foundation(2017T100809); the Key Program of Logistics Research (BWS17J030).

ACKNOWLEDGMENTS

This work was supported by the Postdoctoral Science Foundation(2017T100809); the Key Program of Logistics Research (BWS17J030).

AUTHOR CONTRIBUTIONS

Dapeng Wang, Yinghua Guo and Yuan Liu performed the experiments, analyzed the data, prepared figures and/or tables, and authored or reviewed drafts of the manuscript. Bin Zhang, Po Bai and Xiaolei Su performed the experiments and contributed reagents/materials/analysis tools. Xuege Jiang, Sarengerile Han, Tingzheng Fang, Xuelin Zhang and Diangeng Li performed the experiments and prepared figures and/or tables. Junfeng Wang conceived and designed the experiments, authored or reviewed drafts of the manuscript, and approved the final manuscript draft. Changting Liu conceived and designed the experiments, authored or reviewed drafts of the manuscript, and approved the final manuscript draft.

References

1. Jemal A, Bray F, Center MM, Ferlay J, Ward E, Forman D. Global cancer statistics. CA: A Cancer Journal for Clinicians. 2011;61(2):69-90. https://doi.org/10.3322/caac.20107.
2. Hoffman PC, Mauer AM, Vokes EE. Lung cancer. Lancet. 2000;355(9202):479-85. https://doi.org/10.1016/S0140.
3. Wang R, Ma L, Weng D, Yao J, Liu X, Jin F. Gallic acid induces apoptosis and enhances the anticancer effects of cisplatin in human small cell lung cancer H446 cell line via the ROS-dependent mitochondrial apoptotic pathway. Oncology Reports. 2016;35(5):3075-83. https://doi.org/10.3892/or.2016.4690.
4. Choi HJ, Song JH, Bhatt LR, Baek SH. Anti-human rhinovirus activity of gallic acid possessing antioxidant capacity. Phytotherapy Research. 2010;24(9):1292-6. https://doi.org/10.1002/ptr.3101.
5. Pal C, Bindu S, Dey S, Alam A, Goyal M, Iqbal MS, et al. Gallic acid prevents nonsteroidal anti-inflammatory drug-induced gastropathy in rat by blocking oxidative stress and apoptosis. Free Radical Biology & Medicine. 2010;49(2):258-67. https://doi.org/ 10.1016/j.freeradbiomed.
6. Giftson JS, Jayanthi S, Nalini N. Chemopreventive efficacy of gallic acid, an antioxidant and anticarcinogenic polyphenol, against 1,2-dimethyl hydrazine induced rat colon carcinogenesis. Investigational New Drugs. 2010;28(3):251-9. https://doi.org/10.1007/s10637-009-9241-9.
7. Kaur M, Velmurugan B, Rajamanickam S, Agarwal R, Agarwal C. Gallic acid, an active constituent of grape seed extract, exhibits anti-proliferative, pro-apoptotic and anti-tumorigenic effects against

prostate carcinoma xenograft growth in nude mice. Pharmaceutical Research. 2009;26(9): 2133-40. https://doi.org/10.1007/s11095-009-9926-y.

8. Agarwal C, Tyagi A, Agarwal R. Gallic acid causes inactivating phosphorylation of cdc25A/cdc25C-cdc2 via ATM-Chk2 activation, leading to cell cycle arrest, and induces apoptosis in human prostate carcinoma DU145 cells. Molecular Cancer Therapeutics. 2006;(12):3294-302. https://doi.org/10.1158/1535-7163.
9. Veluri R, Singh RP, Liu Z, Thompson JA, Agarwal R, Agarwal C. Fractionation of grape seed extract and identification of gallic acid as one of the major active constituents causing growth inhibition and apoptotic death of DU145 human prostate carcinoma cells. Carcinogenesis. 2006;27(7):1445-53. https://doi.org/10.1093/carcin/bgi347.
10. Kawada M, Ohno Y, Ri Y, Ikoma T, Yuugetu H, Asai T, et al. Anti-tumor effect of gallic acid on LL-2 lung cancer cells transplanted in mice. Anti-cancer drugs. Anticancer Drugs. 2001;12 (10):847-52. https://doi.org/10.1097/00001813-200111000-00009.
11. Hsu JD, Kao SH, Ou TT, Chen YJ, Li YJ, Wang CJ. Gallic acid induces G2/M phase arrest of breast cancer cell MCF-7 through stabilization of p27(Kip1) attributed to disruption of p27(Kip1)/Skp2 complex. Journal of Agricultural & Food Chemistry. 2011;59(5):1996-2003. https://doi.org/10.1021/jf103656v.
12. Zhao B, Hu M. Gallic acid reduces cell viability, proliferation, invasion and angiogenesis in human cervical cancer cells. Oncology Letter. 2013;6(6):1749-55.
13. You BR, Kim SZ, Kim SH, Park WH. Gallic acid-induced lung cancer cell death is accompanied by ROS increase and glutathione depletion. Molecular and cellular biochemistry. 2011;357(1-2):295-303. https://doi.org/10.1007/s11010-011-0900-8.
14. Russell LH, Mazzio E, Badisa RB, Zhu ZP, Agharahimi M, Oriaku ET, et al. Autoxidation of gallic acid induces ROS-dependent death in human prostate cancer LNCaP cells. Anticancer Research. 2012;32(5):1595-602.
15. Cui S, Xiong L, Lou Y, Shi H, Gu A, Zhao Y, et al. Chu T, Wan. Factors that predict progression-free survival in Chinese lung adenocarcinoma patients treated with epidermal growth factor receptor tyrosine kinase inhibitors. Journal of Thoracic Disease. 2016;8(1):68-78. https://doi.org/10.3978/j.issn.2072-1439.
16. Shi Y, Zhang L, Liu X, Zhou C, Zhang L, Zhang S, et al. Icotinib versus gefitinib in previously treated advanced non-small-cell lung cancer (ICOGEN): a randomised, double-blind phase 3 non-inferiority trial. Lancet Oncology 2013;14(10):953-61. https://doi.org/10.1016/S1470-2045(13)70355-3.
17. Xie J, Liu J, Liu H, Liang S, Lin M, Gu Y, et al. The antitumor effect of tanshinone IIA on anti-proliferation and decreasing VEGF/VEGFR2 expression on the human non-small cell lung cancer A549 cell line. Acta Pharmaceutica Sinica B. 2015;5(6):554-63. Doi: 10.1016/j.apsb.2015.07.008.
18. Zhang T, Ma L, Wu P, Li W, Li T, Gu R, et al. Gallic acid has anticancer activity and enhances the anticancer effects of cisplatin in non-small cell lung cancer A549 cells via the JAK/STAT3 signaling pathway. Oncology reports. 2019;41(3):1779-1788. https://doi.org/10.3892/or.2019.6976.

19. Jiang J, Liang X, Zhou X, Huang R, Chu Z. A meta-analysis of randomized controlled trials comparing carboplatin-based to cisplatin-based chemotherapy in advanced non-small cell lung cancer. Lung Cancer. 2007;57(3):348-58. https://doi.org/10.1016/j.lungcan.
20. Shi Y, Zhang L, Liu X, Shi Y, Zhou C, Zhang L, et al. Icotinib versus gefitinib in previously treated advanced non-small-cell lung cancer (ICOGEN): a randomised, double-blind phase 3 non-inferiority trial. Lancet Oncology. 2011, 14(10):953-61. https://doi.org/10.1016/S1470-2045(13)70355-3.
21. Farabegoli F, Papi A, Bartolini G, Ostan R, Orlandi M. (-)-Epigallocatechin-3-gallate downregulates Pg-P and BCRP in a tamoxifen resistant MCF-7 cell line. Phytomedicine. 2010;7(5):356-362. https://doi.org/10.1016/j.phymed.
22. Pimentel AA, Benaim G. Ca^{2+} and sphingolipids as modulators for apoptosis and cancer. Investigación clínica. 2012;53(1):84-110.
23. Bigler D, Gioeli D, Conaway MR, Weber MJ, Theodorescu D. Rap2 regulates androgen sensitivity in human prostate cancer cells. The Prostate. 2007;67(14):1590-9. https://doi.org/10.1002/pros.20644.
24. Sasaki H. Roles and regulations of Hippo signaling during preimplantation mouse development. Development, Growth & Differentiation. 2017;59(1):12–20. https://doi.org/10.1111/dgd.12335.
25. Zhao B, Tumaneng K, Guan KL. The hippo pathway in organ size control, tissue regeneration and stem cell self-renewal. Nature cell biology. 2011;13(8):877-83. https://doi.org/10.1038/ncb2303.
26. Liu M, Zhao S, Lin Q, Wang XP. YAP regulates the expression of Hoxa1 and Hoxc13 in mouse and human oral and skin epithelial tissues. Molecular and cellular biology. 2015;35(8):1449-61. https://doi.org/10.1128/MCB.00765-14.
27. Harvey K, Tapon N. The Salvador-Warts-Hippo pathway-an emerging tumor-suppressor network. Nature reviews Cancer. 2007;7(3):182-91. https://doi.org/10.1038/nrc2070.

Tables

Table 1. Primers for the target genes used in qPCR

Gene Name	Size（bp）		Primers Sequences (5' to 3')
ACTB	131	Forward	GCCAACACAGTGCTGTCTGG
		Reverse	GAGTACTTGCGCTCAGGAGGAG
Caspase-3	100	Forward	GGTTCATCCAGTCGCTTTGT
		Reverse	AATTCTGTTGCCACCTTTCG
Caspase-9	121	Forward	CTAGTTTGCCCACACCCAGT
		Reverse	TGCTCAAAGATGTCGTCCAG
YAP	91	Forward	GCAGTTGGGAGCTGTTTCTC
		Reverse	CTGTCGAAGATGCTGAGCTG
Cox-2	91	Forward	GCAATAACGTGAAGGGCTGT
		Reverse	CGGGAAGAACTTGCATTGAT
Bcl-2	119	Forward	GAGGATTGTGGCCTTCTTTG
		Reverse	GCCGGTTCAGGTACTCAGTC

Table 2. The expression of key gene in 6 cases of lung adenocarcinoma

Proteins	Scores for the expressed protein level in	
	lung adenocarcinoma tissues	adjacent normal lung tissues
Caspase-3	0	1
Caspase-9	0	4
Bcl-2	0	4
Cox-2	1	2
YAP	0	2
p-YAP	3	1

The expressed protein level was scored according to the immunohistochemical staining scoring standard. The data indicate that the level of Caspase-3, Caspase-9, Bcl-2, Cox-2 and YAP proteins was lower in the non-small cell lung cancer (NSCLC) lung adenocarcinoma tissues than in the paired adjacent normal lung tissues, while the level of p-YAP protein was higher in the NSCLC lung adenocarcinoma tissues than in the paired adjacent normal lung tissues.

Table 3 The inhibitory effect of GA, IH and the GA+IH combination on the PC9 xenograft growth in nude mice.

Groups	Tumor volume (mm3)	Inhibition rate (%)
Control	3423.96±361.57	——
GA	2684.70±790.98*	21.59
IH	2768.95±376.09*	19.13
GA+IH	2283.81±580.96**, #, Δ	33.30

The PC9 xenograft-carrying nude mice were administered with GA (30 μg/kg), IH (100 mg/kg) and GA+IH (30 μg/kg+100 mg/kg), once a day for continuous 14 days, and the PC9 xenograft tumor volume was measured after last drug administration on the 14th day of drug administration. Data are represented as the mean ± SD (n=6). *$P<0.05$, vs the control group, **$P<0.01$, vs the control group; $^{\#}P<0.05$, vs the GA group; $^{\Delta}P<0.05$, vs the IH group.

Table 4. The effect of GA, IH and GA+IH on the serum alanine aminotransferase (ALT) and alkaline phosphatase (ALP) as well as the blood urea nitrogen (BUN) and creatinine (Cr) levels in the PC9 xenograft tumor-bearing nude mice *in vivo* test.

Group	n	ALT (U/L)	ALP (U/L)	BUN (mmol/L)	Cr (μmol/L)
Control	6	1500.0±0***	105.0±7.0***	9.5±0.6**	64±1.5**
GA-30 ug/kg	6	$901.0\pm23.2^{\#\#\#}$	$61.4\pm1.1^{\#\#\#}$	$7.3\pm0.4^{\#}$	$62.4\pm2.1^{\#\#}$
IH-100 mg/kg	6	$852.6\pm30.8^{\Delta\Delta\Delta}$	$62.8\pm1.9^{\Delta\Delta\Delta}$	$7.1\pm0.5^{\Delta}$	59.8±4.4
GA+IH-30ug/kg+100 mg/kg	6	579.4±50.4	58.0±3.8	6.9±0.5	56.4±3.4

The PC9 xenograft tumor-bearing nude mice were administered with GA (30 μg/kg), IH (100 mg/kg) and GA+IH (30 μg/kg+100 mg/kg), all once a day for continuous 14 days, and the serum ALT and ALP as well as the BUN and Cr levels were measured after last drug administration on the 14th day of drug administration. Data are represented as the mean ± SD (n=6). *$P<0.05$, vs the control group, **$P<0.01$, vs the control group; ***$P<0.001$, vs the control group; $^{\#}P<0.05$, vs the GA group; $^{\#\#}P<0.05$, vs the GA group; $^{\#\#\#}P<0.05$, vs the GA group; $^{\Delta}P<0.05$, vs the IH group; $^{\Delta\Delta}P<0.05$, vs the IH group; $^{\Delta\Delta\Delta}P<0.05$, vs the IH group.

Figures

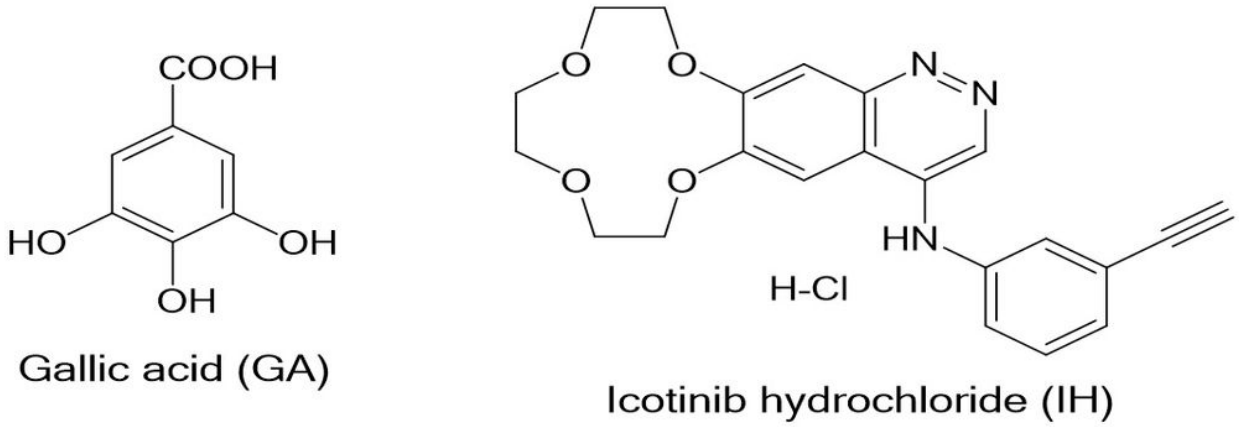

Figure 1

Chemical structure of GA (provided by SIGMA USA). Molecular formula: C7H6O5; Chemical structure of IH (provided by Zhejiang Beta Pharma Co. China). Molecular formula: C22H21N3O4.

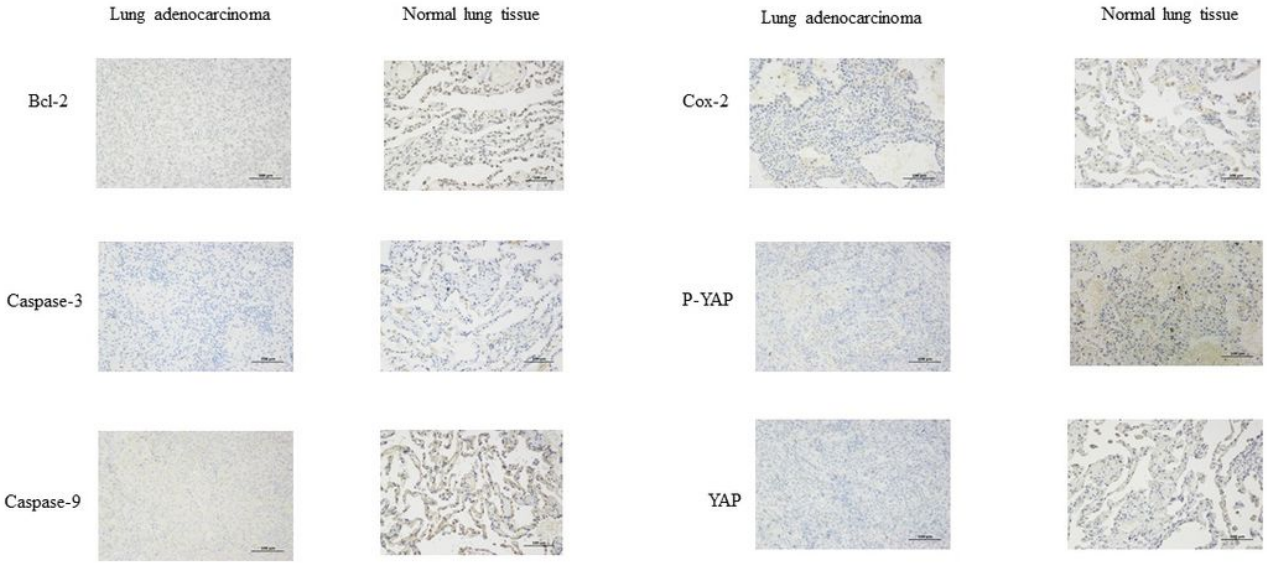

Figure 2

Representative photographs for the immunohistochemical staining of human non-small cell lung cancer lung adenocarcinoma tissues (left column) and paired adjacent normal lung tissues (right column) to examine the Caspase-3, Caspase-9, Bcl-2, Cox-2, YAP and p-YAP expression (×200).

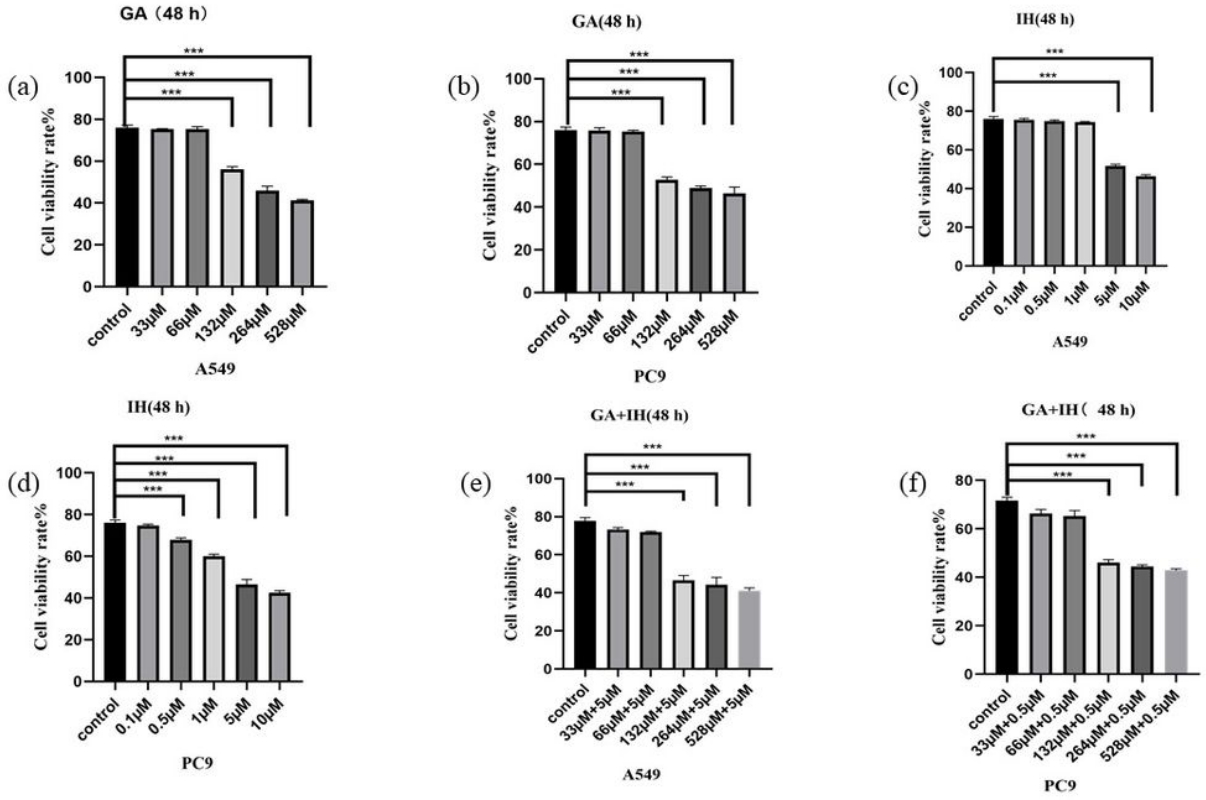

Figure 3

The effect of GA, IH and GA+IH combination on the proliferation of human NSCLC A549 and PC9 cells. (a): Dose-effect curves of GA on A549 and PC9 cells. (b): Dose-effect curves of IH on A549 and PC9 cells. (c-d): Bar graphs for the effect of GA+IH combination on A549 and PC9 cells. (e-f): Bar graphs for the effect of GA+IH combination on A549 and PC9 cells. The A549 and PC9 cells were treated with GA, IH and GA+IH combination at their given concentrations for 48 hr, respectively, and then the cell viability was assayed by the MTT method. The data were normalized with vehicle-treated control cells and are represented as the mean ± SD (n=3). *P<0.05, vs the control group; **P<0.01, vs the control group; ***P<0.001, vs the control group.

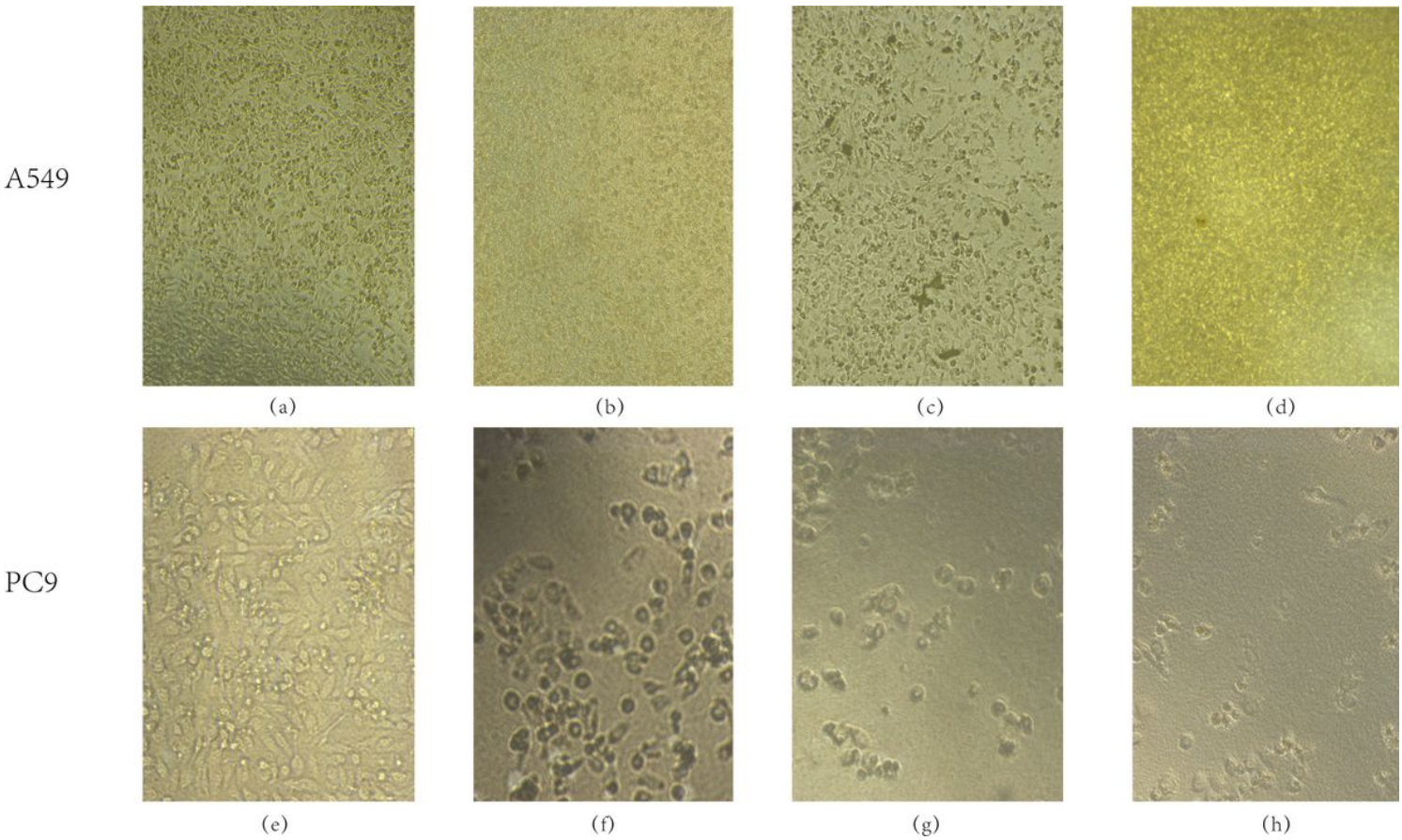

Figure 4

Cellular morphological observations of A549 (a–d,10×) and PC9 (e–h,20×) cells after exposure to drugs for 48 hr. The A549 cells were treated with vehicle using as control (a), 132 μM GA (b), 5 μM IH (c) and 132 μM GA + 5 μM IH (d), while the PC9 cells with vehicle using as control (e), 132 μM GA (f), 0.5 μM IH (g) and 132 μM GA + 0.5 μM IH (h), all for 48 hr respectively, and then the cells were photographed under an inversed phase light microscope.

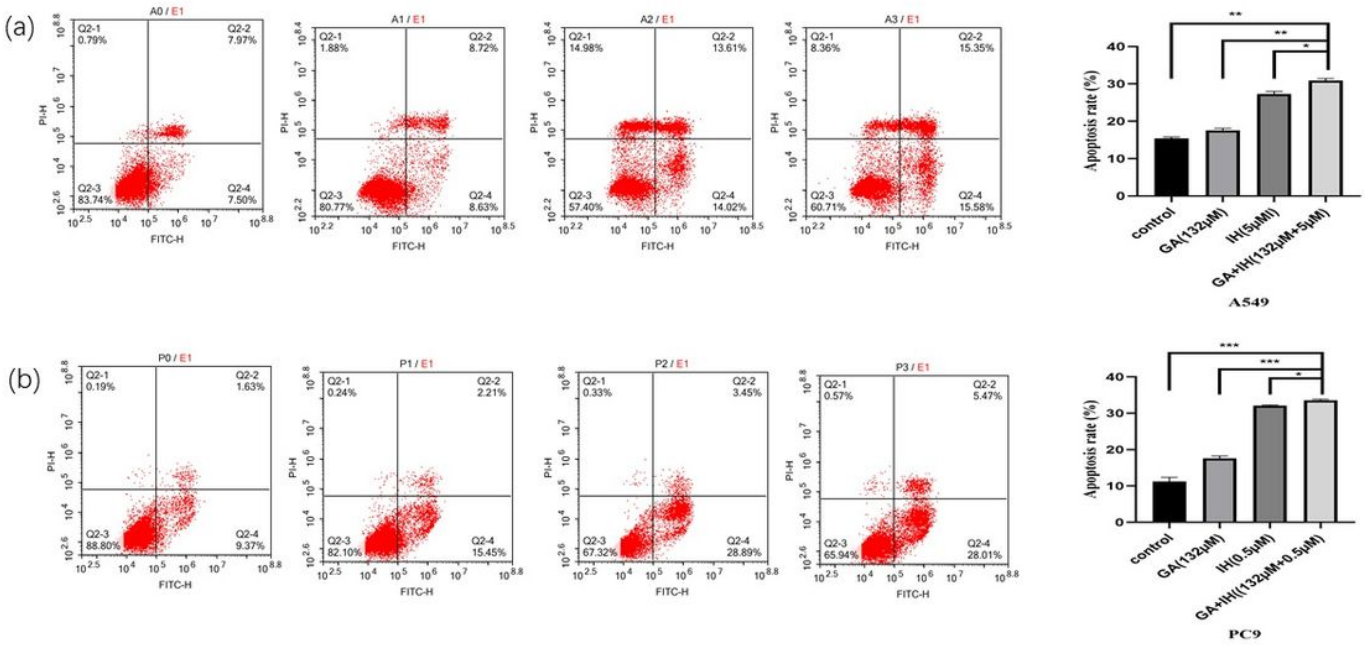

Figure 5

Flow cytometric analysis of apoptosis in A549 (a) and PC9 (b) cells treated with GA, IH and GA+IH for 48 hr. After treatment with the drugs, the cells were stained with Annexin V-FITC and propidium iodide (PI) and then analyzed by flow cytometry. Window areas Q2-1, Q2-2, Q2-3 and Q2-4 in each square graph involve the late apoptotic or dead cells, metaphase apoptotic cells, normal cells and early apoptotic cells, respectively. Bar graph in the right of the graphs (a) and (b) shows the percentage of total apoptotic cells in each group. The data are represented as the mean ± SD (n=3). *P<0.05, **P<0.01, ***P<0.001.

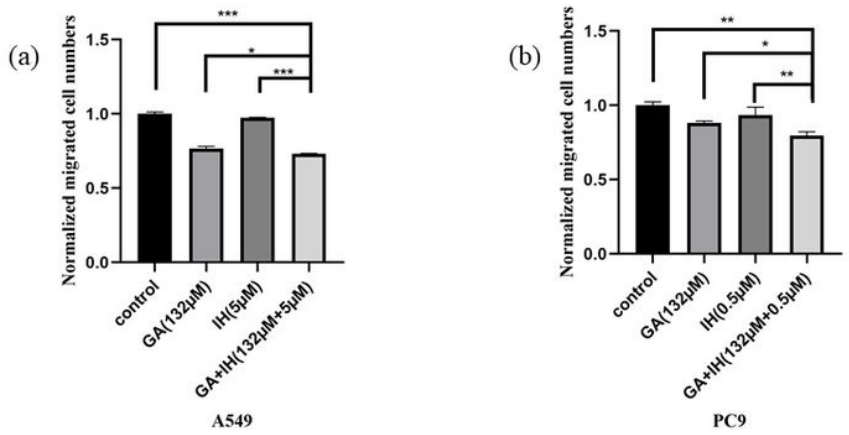

Figure 6

Inhibitory effect of GA, IH and GA+IH on the cell migration of A549 (a) and PC9 (b) cells in Traswell migration assay. After cells were treated with drugs for 48 hr, the migrated cells to the underside of the membrane were stained with crystal violet. To the stained cells, a 33% acetic acid solution was added to dissolve the crystal violet, and then the optical density (OD) at 570 nm was measured on a microplate reader. Migrated cell numbers were calculated according to the OD values and normalized with the cell numbers of control group. Data are represented as the mean ± SD (n=3). *P<0.05, **P<0.01, ***P<0.001.

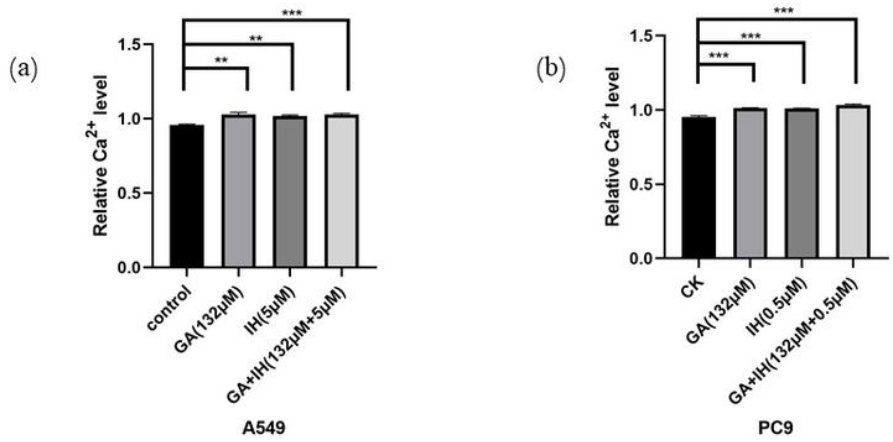

Figure 7

The effect of GA, IH and GA+IH on the intracellular Ca2+ level in A549 (A) and PC9 (B) cells. After treated with drugs for 48 hr, the cells were loaded with Fluo-4 AM, and the intracellular Ca2+ level was determined by the flow cytometry. Data are represented as the mean ± SD (n=3). **P<0.01, vs the control group; ***P<0.001, vs the control group.

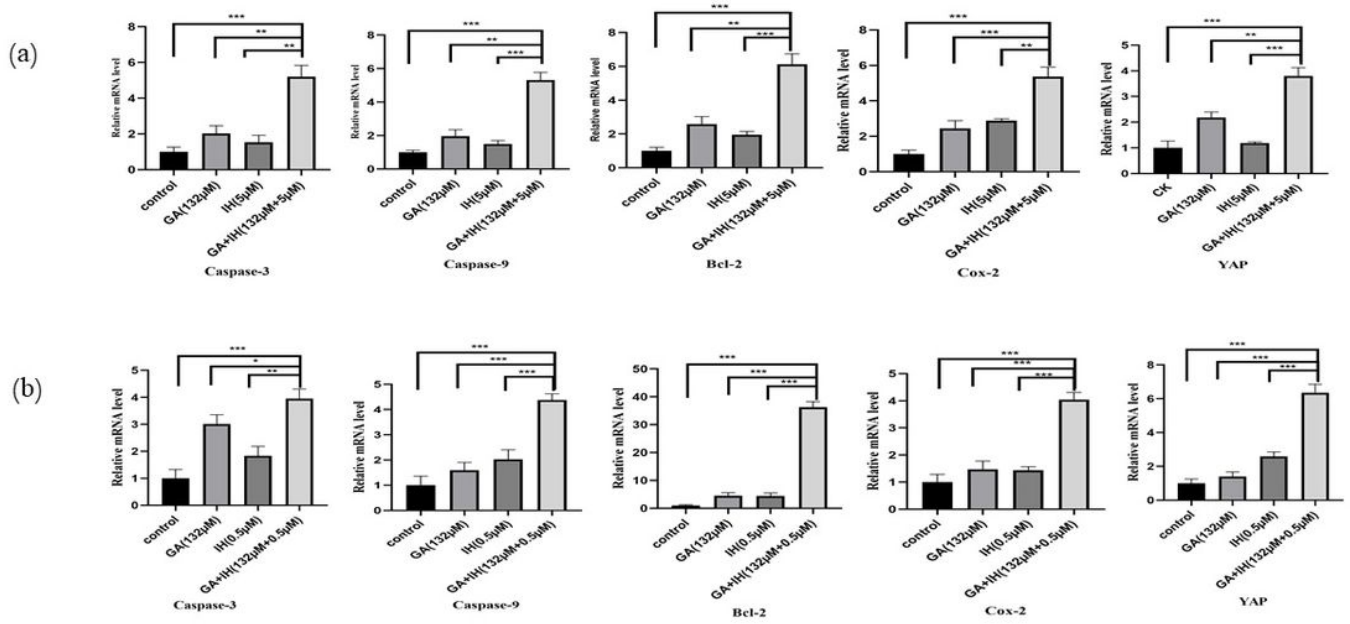

Figure 8

The effect of GA, IH and GA+IH on the expression of Caspase-3, Caspase-9, Cox-2, Bcl-2 and YAP genes at the transcript mRNA level in A549 (a) and PC9 (b) cells. After treatment of the cells with drugs for 48 hr, the relative transcript mRNA level of the genes was quantified by the quantitative RT-PCR analysis using the 2−ΔΔCt method. The mRNA level was normalized with the corresponding control group level, and the data are represented as the mean ± SD (n=3). *P<0.05, **P<0.01, ***P<0.001.

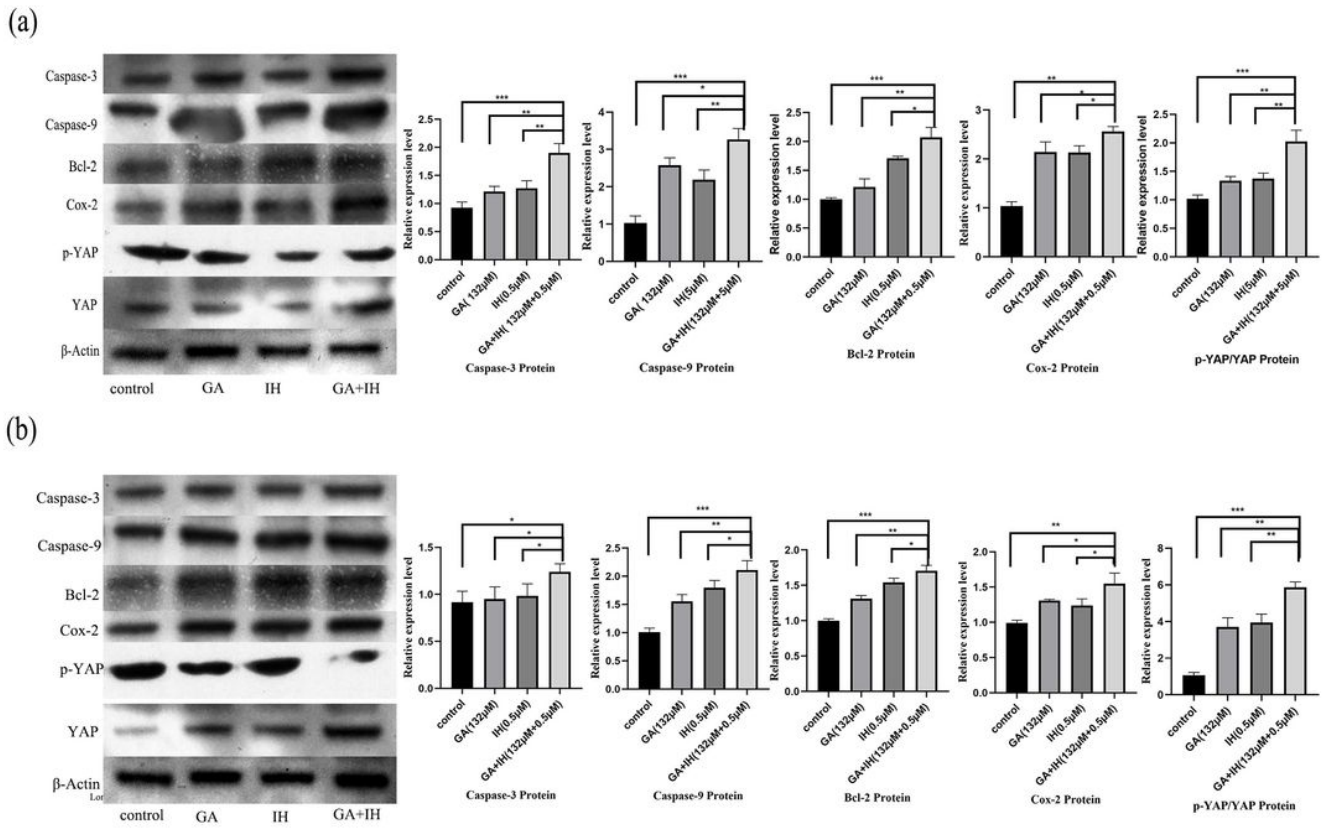

Figure 9

The effect of GA, IH and GA+IH on the Caspase-3, Caspase-9, Bcl-2, Cox-2 and YAP protein expression in A549 (a) and PC9 (b) cells. After treatment of the cells with drugs for 48 hr, the expression of the targeted proteins was examined and quantified by the Western blot analysis. The β-actin was used as the loading control. The relative expression level of the targeted proteins was normalized with the corresponding control group level. Data are represented as the mean ± SD (n=3). *P<0.05, **P<0.01, ***P<0.001, ***P<0.001.

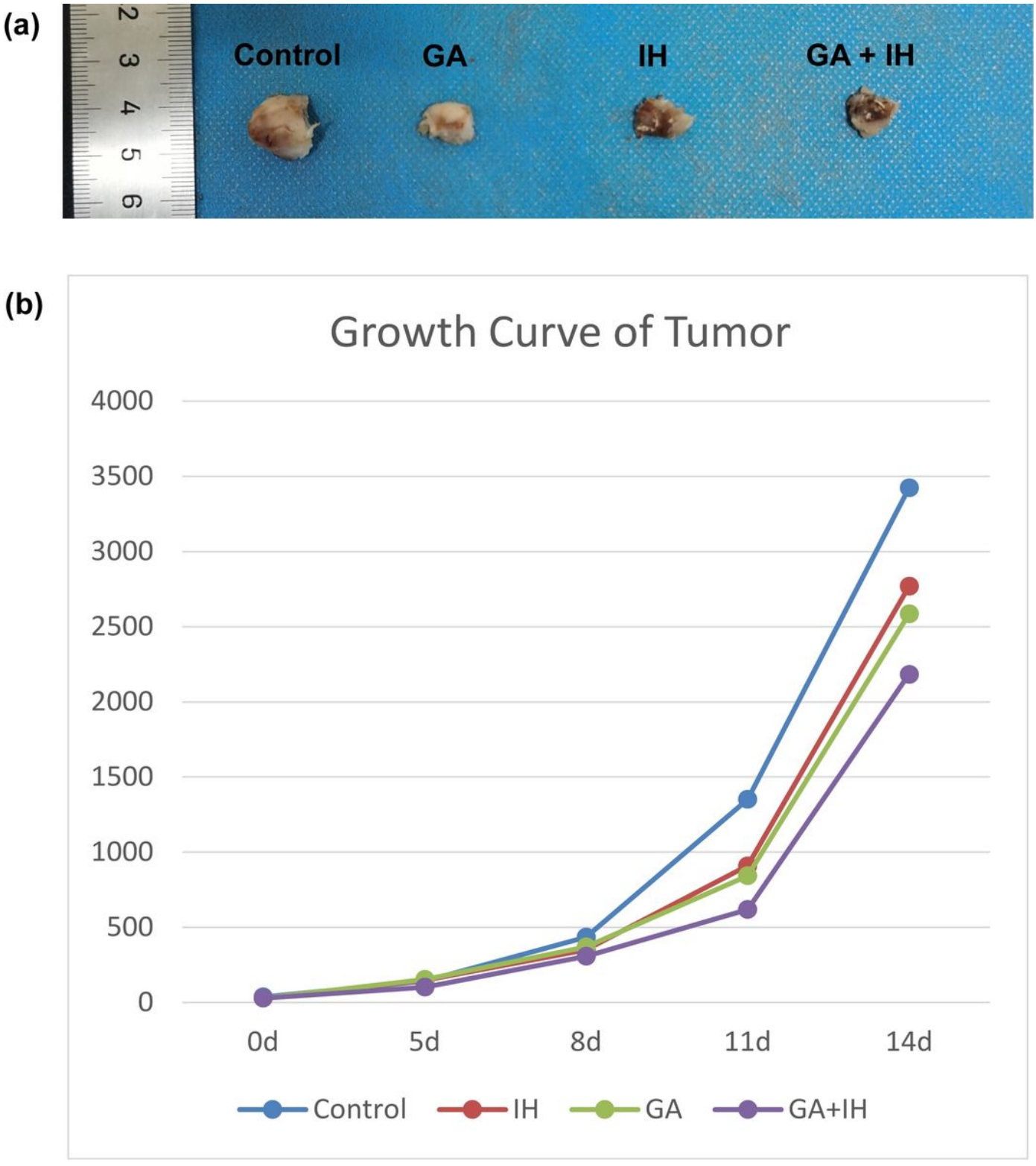

Figure 10

The inhibition of PC9 xenograft growth in nude mice by GA (30 μg/kg), IH (100 mg/kg) and GA+IH (30 μg/kg+100 mg/kg) administered once a day for continuous 14 days. (a): Representative images of the PC9 xenograft tumors in each group on the 14th day of drug administration; (b): Time course curves of the PC9 xenograft tumor growth for each group.

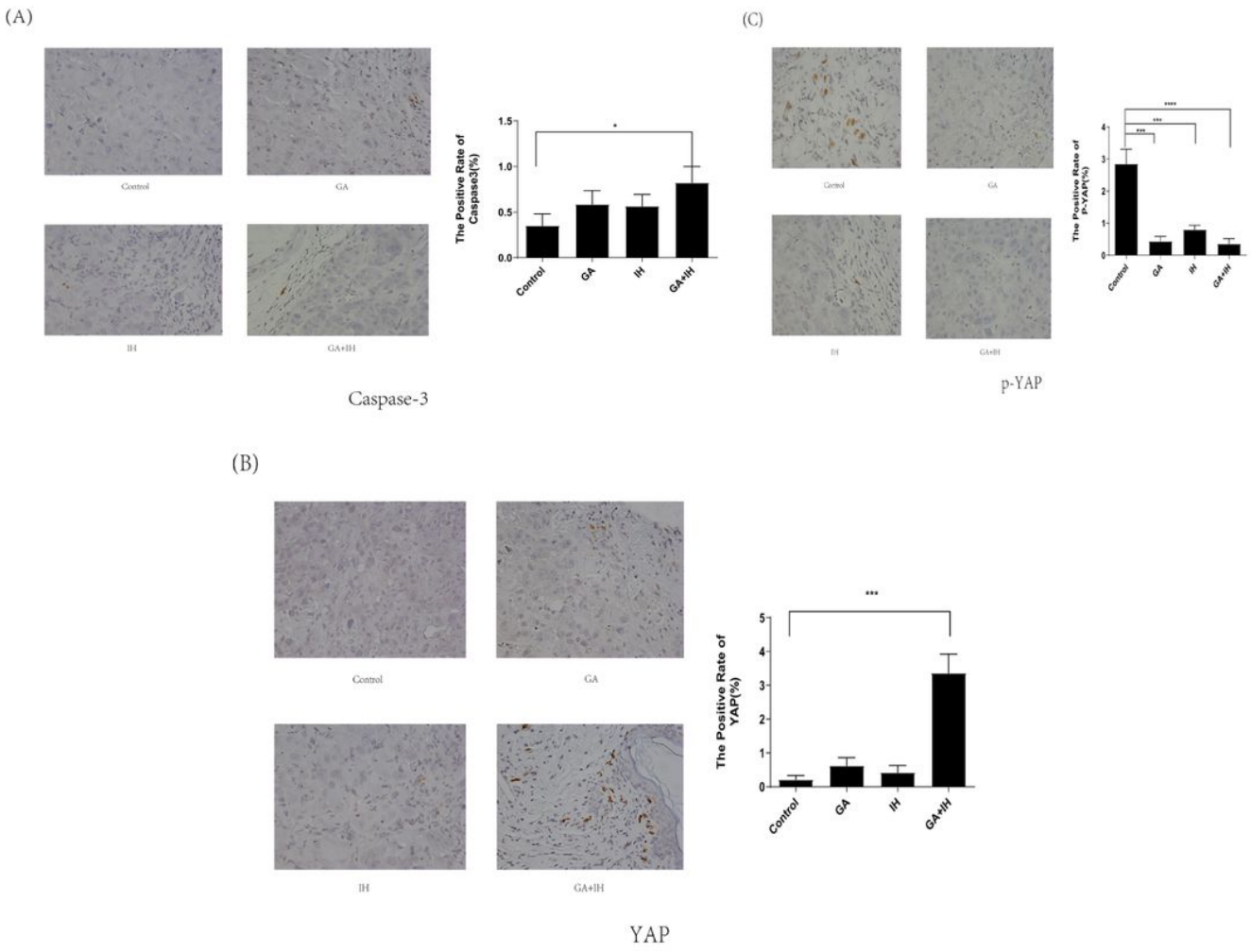

Figure 11

The effect of GA, IH and GA+IH on the expression of Caspase-3, YAP and p-YAP proteins in mouse tumor tissues in the A549 xenograft tumor-bearing nude mice in vivo test. The tumor-bearing mice were administered with GA (30 μg/kg), IH (100 mg/kg) and GA+IH (30 μg/kg+100 mg/kg), each once a day for continuous 14 days, and the tumors were taken out after last drug administration on the 14th day of drug administration. The expressed Caspase-3 (A), YAP (B) and p-YAP (C) proteins in the tumor tissues were visualized by the immunohistochemical staining of the tumor tissues with the corresponding antibody, respectively, and the percentage of the positively stained proteins was measured by the immunohistochemistry method. Photos show the image of immunohistochemical staining of the tumor tissues (×400). Bar graphs show the percentage of corresponding proteins positively stained.